cmgh
CELLULAR AND MOLECULAR GASTROENTEROLOGY AND HEPATOLOGY

ORIGINAL RESEARCH

Defects in NADPH Oxidase Genes *NOX1* and *DUOX2* in Very Early Onset Inflammatory Bowel Disease

Q10 Patti Hayes,[1,*] Sandeep Dhillon,[2,3,*,§] Kim O'Neill,[1,*] Cornelia Thoeni,[2,3,§] Ken Y. Hui,[4] Abdul Elkadri,[2,3,§] Conghui H. Guo,[2,3,§] Lidija Kovacic,[1] Gabriella Aviello,[1] Luis A. Alvarez,[5] Anne M. Griffiths,[3,§] Scott B. Snapper,[6,§] Steven R. Brant,[7] James H. Doroshow,[8] Mark S. Silverberg,[9] Inga Peter,[10] Dermot P. B. McGovern,[11] Judy Cho,[12] John H. Brumell,[2,§] Holm H. Uhlig,[13] Billy Bourke,[1,5,*,§] Aleixo A. Muise,[2,3,*,§] and Ulla G. Knaus[1,5,*]

[1]*Conway Institute, School of Medicine, University College Dublin, Dublin, Ireland;* [2]*SickKids Inflammatory Bowel Disease Center and Cell Biology Program, Research Institute, Hospital for Sick Children, Toronto, Ontario, Canada;* [3]*Division of Gastroenterology, Hepatology, and Nutrition, Department of Pediatrics, University of Toronto, Hospital for Sick Children, Toronto, Ontario, Canada;* [4]*Program in Computational Biology and Bioinformatics, Yale University, New Haven, Connecticut;* [5]*National Children's Research Centre, Our Lady's Children's Hospital Crumlin, Dublin, Ireland;* [6]*Division of Pediatric Gastroenterology, Hepatology, and Nutrition, Department of Medicine, Children's Hospital Boston; Division of Gastroenterology and Hepatology, Brigham & Women's Hospital, Department of Medicine, Harvard Medical School, Boston, Massachusetts;* [7]*Harvey M. and Lyn P. Meyerhoff Inflammatory Bowel Disease Center, Department of Medicine, School of Medicine and the Department of Epidemiology, Bloomberg School of Public Health, Johns Hopkins University, Baltimore, Maryland;* [8]*National Cancer Institute, National Institutes of Health, Bethesda, Maryland;* [9]*Mount Sinai Hospital Inflammatory Bowel Disease Group, University of Toronto, Zane Cohen Centre for Digestive Diseases, Toronto, Ontario, Canada;* [10]*Department of Genetics and Genomic Sciences, Icahn School of Medicine at Mount Sinai, New York, New York;* [11]*F. Widjaja Foundation Inflammatory Bowel and Immunobiology Research Institute, Cedars-Sinai Medical Center, Los Angeles, California;* [12]*Section of Gastroenterology, Department of Internal Medicine, Icahn School of Medicine at Mount Sinai, New York, New York;* [13]*Translational Gastroenterology Unit, Nuffield Department of Clinical Medicine and Children's Hospital, John Radcliffe Hospital, University of Oxford, Oxford, United Kingdom*

Q2 **SUMMARY**

NOX1 and *DUOX2* are the first inactivating missense variants to be associated with very early onset inflammatory bowel disease (VEOIBD). Defective reactive oxygen species production from intestinal epithelial cells constitutes a risk factor for VEOIBD development.

Q3 **BACKGROUND & AIMS:** Defects in intestinal innate defense systems predispose patients to inflammatory bowel disease (IBD). Reactive oxygen species (ROS) generated by nicotinamide-adenine dinucleotide phosphate (NADPH) oxidases in the mucosal barrier maintain gut homeostasis and defend against pathogenic attack. We hypothesized that molecular genetic defects in intestinal NADPH oxidases might be present in children with IBD.

METHODS: After targeted exome sequencing of epithelial NADPH oxidases *NOX1* and *DUOX2* on 209 children with very early onset inflammatory bowel disease (VEOIBD), the identified mutations were validated using Sanger Sequencing. A structural analysis of *NOX1* and *DUOX2* variants was performed by homology in silico modeling. The functional characterization included ROS generation in model cell lines and in in vivo transduced murine crypts, protein expression, intracellular localization, and cell-based infection studies with the enteric pathogens *Campylobacter jejuni* and enteropathogenic *Escherichia coli*.

RESULTS: We identified missense mutations in *NOX1* (c.988G>A, p.Pro330Ser; c.967G>A, p.Asp360Asn) and *DUOX2* (c.4474G>A, p.Arg1211Cys; c.3631C>T, p.Arg1492Cys) in 5 of 209 VEOIBD patients. The *NOX1* p.Asp360Asn variant was replicated in a male Ashkenazi Jewish ulcerative colitis cohort. All *NOX1* and *DUOX2* variants showed reduced ROS production compared with wild-type enzymes. Despite appropriate cellular localization and comparable pathogen-stimulated translocation of altered oxidases, cells harboring *NOX1* or *DUOX2* variants had defective host resistance to infection with *C. jejuni*.

CONCLUSIONS: This study identifies the first inactivating missense variants in *NOX1* and *DUOX2* associated with VEOIBD. Defective ROS production from intestinal epithelial cells constitutes a risk factor for developing VEOIBD. *(Cell Mol Gastroenterol Hepatol 2015;■:■–■; http://dx.doi.org/10.1016/j.jcmgh.2015.06.005)*

Keywords: Inflammatory Bowel Disease; NADPH Oxidase; *NOX1*; *DUOX2*; Reactive Oxygen Species; VEOIBD.

*Authors contributed equally to the study; §Participant in the International Early Onset Pediatric IBD Cohort Study (www.NEOPICS.org).

Abbreviations used in this paper: **AJ, Ashkenazi Jewish; CGD, chronic granulomatous disease; *DUOX2*, dual oxidase 2; HA, human influenza hemagglutinin; IBD, inflammatory bowel disease; FAD, flavin adenine nucleotide; MAF, minor allele frequency; NADPH, nicotinamide-adenine dinucleotide phosphate; *NOX1*, NADPH oxidase 1; PAS, periodic acid–Schiff; PBS, phosphate-buffered saline; PMA, phorbol 12-myristate 13-acetate; ROS, reactive oxygen species; SNP, single-nucleotide polymorphism; UC, ulcerative colitis; VEOIBD, very early onset inflammatory bowel disease; WT, wild type.**

2352-345X
http://dx.doi.org/10.1016/j.jcmgh.2015.06.005

Inflammatory bowel disease (IBD), a complex disease associated with genetic predisposition and environmental factors, is characterized by recurrent intestinal inflammation and microbial dysbiosis. Genomewide association studies link adult IBD to alterations in genes involved in host-microbe interactions.[1,2] Nicotinamide adenine dinucleotide phosphate (NADPH) oxidase-generated reactive oxygen species (ROS) are intrinsic to the antimicrobial host defense system of professional phagocytes. Defective ROS production in patients with chronic granulomatous disease (CGD), a rare genetic disorder caused by inactivating alterations of genes required for formation of the penultimate phagocyte oxidase complex (*CYBB*, *CYBA*, *NCF1*, *NCF2*, *NCF4*), confers susceptibility to life-threatening bacterial and fungal infections.[3] Up to 40% of CGD patients develop inflammatory colitis that mimics Crohn's disease.[4] Genetic variants in *NCF4* and *NCF2* that lead to partial attenuation in phagocyte oxidase (NADPH oxidase 2, *NOX2*) function without causing CGD have been associated with adult and very early onset IBD (VEOIBD).[5,6] We have recently shown that single-nucleotide polymorphisms (SNPs) and rare hypomorphic variants in all components of the NOX2 NADPH oxidase complex are associated with VEOIBD.[7]

A role for ROS production by intestinal epithelial cells in mucosal barrier function and intestinal homeostasis is just emerging.[8] The predominant source of ROS in the lining of the gastrointestinal tract is the NADPH oxidases NOX1 (NADPH oxidase 1) and DUOX2 (dual oxidase 2), with NOX1 expression restricted mainly to colon, caecum, and ileum, whereas DUOX2 can be found in all segments of the gut.[9] NOX1 and DUOX2 are the catalytic subunits of multimeric, membrane-bound enzymes that generate upon stimulation superoxide and hydrogen peroxide by transfer of electrons from NADPH to molecular oxygen. We[10] and others[11–13] have reported NOX1/DUOX2-mediated ROS production in the intestine and its effect on bacterial pathogenicity and barrier integrity. Here, we describe the identification and characterization of missense mutations in *NOX1* (NM_007052.4, location Xq22) and in *DUOX2* (NG_016992, location 15q15.3) in patients diagnosed with VEOIBD.

Materials and Methods

Study Design

All results are presented according to the STrengthening the REporting of Genetic Association Studies (STREGA) guidelines.[14] Fifty-nine IBD patients diagnosed under the age of 6 years were sequenced for *NOX1* and *DUOX2* by targeted exome sequencing using Agilent SureSelect target enrichment and sequencing (Agilent Technologies, Santa Clara, CA) on the Illumina HiSeq 2000/2500 (Illumina, San Diego, CA) with exon primer and sequencing protocols designed by the Beckman Coulter Genomics (beckmangenomics.com; Beckman Coulter, Brea, CA) as described previously elsewhere.[15] Sanger sequencing was used to verify all genetic defects identified using targeted sequencing of the *NOX1* and *DUOX2* genes at the Centre for Applied Genomics (TCAG; http://www.tcag.ca; Hospital for Sick Children, Toronto, ON, Canada).

Single-nucleotide and insertion/deletion (indel) variants identified by targeted exome sequencing and validated by Sanger sequencing were automatically scanned and manually verified. Furthermore, all variants were also validated using Taqman performed by the Centre for Applied Genomics, Hospital for Sick Children.[15,16] Function and minor allele frequency (MAF) were searched for using the National Heart, Lung, and Blood Institute Exome Sequencing Project (ESP) Exome Variant Server (http://evs.gs.washington.edu/EVS/), the National Center for Biotechnology Information dbSNP (http://www.ncbi.nlm.nih.gov/projects/SNP/), the National Institute of Environmental Health Sciences FuncPred (http://snpinfo.niehs.nih.gov/snpinfo/snpfunc.htm), Polyphen2 (http://genetics.bwh.harvard.edu/pph2/),[17] SIFT (http://sift.jcvi.org/),[18] FastSNP (http://fastsnp.ibms.sinica.edu.tw/),[19] Human Splicing Finder (http://www.umd.be/HSF/),[20] and pfSNP (http://pfs.nus.edu.sg/).[21]

Setting

Patients included in the study were recruited from the Inflammatory Bowel Disease Clinic at the Hospital from Sick Children, University of Toronto. They were diagnosed with VEOIBD between the years 1994 and 2012 and had a confirmed diagnosis of IBD before the age of 6 years. Although there is no consensus on the definition of VEOIBD, we have used the stricter definition based on our recent modification (diagnosis <6 years of age)[5,22,23] of the Paris classification (<10 years of age excluding <2 year old).[24] Our definition, which is more stringent and includes more severe cases that are more likely to cause monogenic forms of the disease, has been used to identify risk variants in this age group. There were no exclusion criteria for patients diagnosed with VEOIBD; however, patients with a known immunodeficiency or a clinical diagnosis of CGD were excluded because these patients were not defined as VEOIBD. The five identified patients were screened and were found negative for pathogenic mutations in *IL10RA*, *L10RB*, *IL10*, *XIAP*, *TTC7A*, as well as genes involved in CGD (*RAC1/2*, *NCF1/2/4*, and *CYBB*)[23,25] and *NOD2* and *ATG16L1* variants associated with IBD.

Participants

This was a cohort study that examined the genetics of VEOIBD patients. Fifty-five VEOIBD patients were recruited from the Hospital for Sick Children, Toronto, Canada. A second cohort of VEOIBD patients was recruited through NEOPICS (www.NEOPICS.org). The replication cohort comprised 1477 Crohn's disease cases, 559 ulcerative colitis cases, and 2614 healthy controls, all with genetically verified Ashkenazi Jewish ancestry by principal components analysis.

Standard quality control procedures were applied, and we performed association testing using Fisher's exact method, stratified by gender in 297 male ulcerative colitis (UC) cases, 262 female UC cases, 1708 male controls, and 906 female controls. Phenotypic information and DNA samples were obtained from the study participants with approval of the institutional review ethics board for IBD

genetic studies at the Hospital for Sick Children and Mount Sinai Hospital Toronto.

Later onset UC cases were recruited through the National Institute of Diabetes and Digestive and Kidney Diseases Inflammatory Bowel Disease Genetics Consortium, the Cedars-Sinai Medical Center IBD Center in California and Mount Sinai Hospital in New York. Replication cohorts had ethics board approval for genetic and phenotypic studies at the individual institutions. Written informed consent was obtained from all participants/parents.

H&E and Periodic Acid–Schiff Staining in Patient Biopsy Samples

Colonic biopsy samples were fixed in 10% formaldehyde without methanol and afterward embedded in paraffin. For H&E staining, embedded paraffin tissues on slides were deparaffinized with xylene and afterward rehydrated with different percentages of ethanol. The slides were stained for 5 minutes with Meyer's hematoxylin (Fisher Scientific, Fair Lawn, NJ) for nuclei and counterstained with eosin-Y (Fisher Scientific) for cytoplasm. Slides were mounted in Entellan (EMD Millipore, Billerica, MA). Photographs were taken using an epifluorescence light microscope (Leica Microsystems, Buffalo Grove, IL) and adjusted for brightness, contrast, and pixel size in Adobe Photoshop CS5 version 12.0 (Adobe System, San Jose, CA).

Modeling and Docking Procedure

Three-dimensional (3D) models of C-terminal domains of *NOX1* and *DUOX2* were generated using the homology modeling program Modeller 9v11 (http://www.salilab.org/modeller/).[26] Blast of PDB was performed with the NOX1 FAD-binding domain, and a combination of several homologous structures served together with the 3D X-ray structure the NOX2 NADPH binding domain (PDB ID: 3A1F) as initial template. The modeling was performed with default parameters using the "allHmodel" protocol to include hydrogen atoms and the "HETATM" protocol to include FAD and NADPH. To compare the FAD and NADPH binding interaction between wild-type (WT) and sequence altered oxidases, the docking runs were performed with HADDOCK.[27,28] Docking was performed with most of the parameters set to default using the Web server version of HADDOCK with a Guru interface. To gain the Van der Waals, electrostatic, and desolvation energy for each enzyme - FAD or -NADPH model, HADDOCK automatically performed the molecular dynamics before and after each docking trial by including water into the calculation (detailed modeling procedure, publication in preparation).

Cell Culture and Transfection

Model cell lines were employed as intestinal epithelial cell lines, and primary colon cells express endogenous NOX1 and DUOX2. Cos7 cells are a suitable model system for NOX1-based oxidase reconstitution as they lack any functional NADPH oxidases, and NCI-H661 cells serve as a physiologically relevant model for DUOX oxidases.[29] Cos7 cells stably expressing $p22^{phox}$ [30] were maintained in Dulbecco's modified Eagle's medium with 10% fetal bovine serum; for NCI-H661 cells stably expressing DUOXA2,[29] RPMI 1640 medium with 10% fetal bovine serum was used. Human *NOX1* was cloned into pcDNA3.1 with and without the N-terminal Myc epitope tag including a linker sequence. Human influenza hemagglutinin (HA)-tagged human DUOX2 in pcDNA3.1 was prepared by cloning the HA tag between amino acids D27 and A28. Mutations were introduced using site-directed mutagenesis and were verified by sequencing. NOX1 WT and missense variants were transiently transfected with NOXA1 and Myc-NOXO1 into Cos-$p22^{phox}$ cells (24 hours). HA-tagged DUOX2 WT and missense variants were transiently transfected into H661-DUOXA2 cells or together with DUOXA2 into Cos7 cells using X-tremeGENE (Roche Applied Science, Indianapolis, IN) (48 hours). For analysis of DUOX2 localization upon bacterial challenge, HT29 colon epithelial cells expressing endogenous NOX1 and NOD2 were stably transduced with lentivirus encoding for HA-tagged DUOX2 WT, DUOX2 R1211C, and DUOX2 R1492C in combination with WT DUOXA2.

Protein Isolation and Western Blotting

Cells were lysed in radioimmunoprecipitation assay buffer and after gel electrophoresis and blotting, membranes were probed with α-HA (Covance Laboratories, Princeton, NJ), α-DUOX2,[31] α-Myc (9E10), α-NOXA1,[31] α-NOX1,[32] α-$p22^{phox}$ FL-195 (Santa Cruz Biotechnology, Dallas, TX), α-calnexin (BD Biosciences, San Jose, CA), and horseradish peroxidase-conjugated anti-rabbit or anti-mouse antibody (SouthernBiotech, Birmingham, AL). Proteins were visualized using electrochemiluminescence reagent (Pierce Biotechnology, Rockford, IL). Immunoblotting of $p22^{phox}$ or calnexin served as control.

ROS Assays

Superoxide production (NOX1) was measured using luminol enhanced chemiluminescence and stimulation with 1 mg/mL phorbol 12-myristate 13-acetate (PMA) for 30 minutes.[33] Luminescence was measured on a Berthold Centro 960 LB in white 96-well plates. The chemiluminescence (relative light units, ΔRLU) readings were standardized against cellular protein (BCA assay).

H_2O_2 production (DUOX2) was measured using the homovanillic acid assay and addition of 1 μM thapsigargin.[34] H_2O_2 production was standardized to H_2O_2 standard curves and cell lysate protein concentration. empty vector transfection served as the control. For crypt ROS assays, $Nox1^{-/-}$ mice (Jackson Laboratory, Bar Harbor, ME) were transduced with lentivirus encoding empty vector, NOX1, NOX1 D330N, and NOX1 P360S. Briefly, the lentiviral titer was determined relative to p24 particles (QuickTiter Lentivirus Titer Kit; Cell Biolabs, San Diego, CA), and equal amounts of each lentivirus were intrarectally administered to $Nox1^{-/-}$ mice. Crypts were isolated from the intestine of euthanized mice 24 hours after lentiviral administration.

PMA-stimulated superoxide production was measured using L-012 enhanced chemiluminescence, and

Table 1. List of Variants Found in *NOX1* and *DUOX2* in Very Early Onset Inflammatory Bowel Disease Patients

Gene	Variant	rs #	MAF/Minor Allele Count*	CADD Rank Score	Age at Diagnosis (y)	Gender	Diagnosis	Patient Summary
NOX1	c.988G>A p.P330S	Novel	Novel—no data available	0.40694	1.8	Male	IBD-U	Severe pancolitis Granuloma
NOX1	c.967G>A p.D360N	rs34688635	T = 0.010/16	0.5415	5.3 4.7	Female Male	UC IBD-U	Pancolitis Pancolitis
DUOX2	c.4474G>A p.R1211C	Novel	Novel—no data available	0.90955	4.7	Male	IBD-U	Severe pancolitis Colectomy, perforation Recurrence of disease
DUOX2	c.3631C>Tpp.R1492C	rs374410986, Novel	Novel—no data available	0.9002	4.3	Male	UC	Pancolitis

Note: CADD, Combined Annotation Dependent Depletion; *DUOX2*, dual oxidase 2; IBD-U, inflammatory bowel disease unclassified; MAF, minor allele frequency; *NOX1*, NADPH oxidase 1; UC, ulcerative colitis.
*The minor allele frequencies are taken from 1000 Genomes of dbSNP.

standardization was performed against total crypt protein concentration, as measured by BCA assay. ROS generation by transduced crypts was performed in two independent experiments (n = 2–3). Animal experiments were performed with ethics approval and authorization by the regulatory authority (HPRA, IE).

Flow Cytometry

H661-DUOXA2 cells expressing DUOX2 WT or variants were incubated with α-HA antibody (Covance Laboratories) in fluorescence-activated cell sorting buffer on ice for 30 minutes without cell permeabilization. After incubation with anti-mouse Alexa Fluor 647, the cells were fixed in 1.5% paraformaldehyde and analyzed on an Accuri C6 flow cytometer (BD Biosciences).

Immunofluorescence

Cells expressing Myc-NOX1 WT or variants were treated with TAMRA-labeled *Campylobacter jejuni* for 15 minutes to visualize localization of NOX1 as described elsewhere[10] while DUOX2-DUOXA2-expressing cells were not stimulated. Cells were fixed in 3% paraformaldehyde, permeabilized in 0.5% Triton X-100, and stained with α-DUOX2 or α-Myc antibody, followed by goat anti-rabbit or anti-mouse Alexa Fluor 488 (Invitrogen/Life Technologies, Carlsbad, CA). HT29 cells expressing DUOX2 WT or missense variants were seeded on glass coverslips and treated with 300 μL of a clinical isolate of enteropathogenic *Escherichia coli* (EPEC) at optical density $OD_{600} = 1$ for 5 hours. Slides were washed, fixed, and permeabilized with 0.1% Triton X-100 and probed with antibodies against HA tag (Covance) and NOD2 (sc-30199, kind gift by P. Moynagh, National University of Ireland Maynooth), and 4′,6-diamidino-2-phenylindole (DAPI, blue). Images were acquired using a Zeiss LSM 700 microscope (Carl Zeiss, Thornwood, NY) and magnification 63× (oil) objective.

Colonic biopsies from control, disease control, and patients were fixed in 10% formaldehyde without methanol, embedded in paraffin, and processed for staining. Antigen retrieval was performed using high pressure-cooking with 1 mM EDTA at a pH 9.0 containing 0.05% Tween 20. Afterward, slides were blocked for 1 hour at room temperature with 5% bovine serum albumin in 1x phosphate-buffered saline (PBS) without calcium and magnesium containing 15% goat serum. Primary antibody incubation was performed overnight at 4°C. On the following day, the stained slides were washed three times for 10 minutes with 1x PBS without calcium and magnesium.

Secondary antibody incubation was performed at room temperature and in darkness for 1 hour. Slides were washed afterward three times for 10 minutes in darkness. Next, nuclear counterstaining with Hoechst 33342 Fluorescence Stain (Thermo Fisher Scientific, Waltham, MA) was performed at a dilution of 1:15,000. Finally, sections were mounted overnight with Vectorshield fluorescence mounting medium (Vector Laboratories, Burlingame, CA). Antibodies α-beta catenin (BD Transduction Laboratories, BD Biosciences), α-lysozyme (Abcam, Cambridge, MA), α-CD24 (Abcam), and α-EpCAM (Sigma-Aldrich, St. Louis, MO) were used at 1:100 dilution. Secondary antibodies were Alexa fluor 568 goat anti-rabbit and Alexa fluor 488 goat-anti mouse (both Invitrogen/Life Technologies). Images were acquired with an Olympus IX81 inverted fluorescence microscope (Olympus America, Center Valley, PA) equipped with a Hamamatsu C9100-13 back-thinned EM-CCD camera (Hamamatsu Photonics KK, Hamamatsu City, Japan) and Yokogawa CSU X1 spinning disk confocal scan head (Yokogawa Electric Corporation, Tokyo, Japan). Images were adjusted for contrast and brightness using the Volocity version 6.1.1 software (PerkinElmer Life and Analytical Sciences, Waltham, MA).

Virulence Assay

Adherence and invasion of *C. jejuni* 81-176 were assessed in NOX1 complex or DUOX2-DUOXA2 expressing Cos7 cells using the gentamicin protection assay.[35] Plate

Table 2. ■■■ Q9

Gene	Variant	Chromosome	Position	rs#	Chromosomal position	Minor Allele Frequency (dbSNP)	Minor Allele Frequency (1000G)	Minor Allele Frequency (NHLBI exome variant frequencies)	ExAC v0.3 MAF	SIFT	SIFT Prediction
NOX1 (Choice 1)	P330S	X	100105285	Novel	c.988G>A	No MAF data	No MAF data	No MAF data	No MAF data	0.051	Tolerated
NOX1	D360N	X	100105195	rs34688635	c.967G>A	T=0.010/16 (1%)	T=0.00529801	0.019881	0.018	0.042	Tolerated
DUOX2	R1211C	15	45389874	rs374410986	c.3631C>T	No MAF data	No MAF data	A=7.7e-05	A=0.00004118	0	Damaging
DUOX2	R1492C	15	45386811	Novel	c.4474G>A	No MAF data	No MAF data	No MAF data	A=0.00004118	0	Damaging

Table 2. Continued

Gene	PolyPhen2	PolyPhen2 Prediction	Mutation Taster	Mutation Taster Prediction	Mutation Assessor	Mutation Assessor Prediction	FATHMM	FATHMM Prediction	LRT Score	LRT Prediction	GERP++	PhyloP	CADD Rank Score
NOX1 (Choice 1)	1	Probably Damaging	1	Disease Causing	3.185	Predicted Functional (Medium)	2.44	Tolerated	0	Deleterious	3.87	1.767	0.40694
NOX1	0.085	Possibly Damaging	0	Polymorphism Automatic	2.225	Predicted Functional (Medium)	-3.09	Damaging	0.000445	Deleterious	3.87	1.767	0.54147
DUOX2	1	Probably Damaging	1	Disease Causing	3.37	Predicted Functional (Medium)			0	Deleterious	5.69	2.679	0.90955
DUOX2	1	Probably Damaging	1	Disease Causing	3.97	Predicted Functional (High)			0	Deleterious	5.68	2.838	0.9002

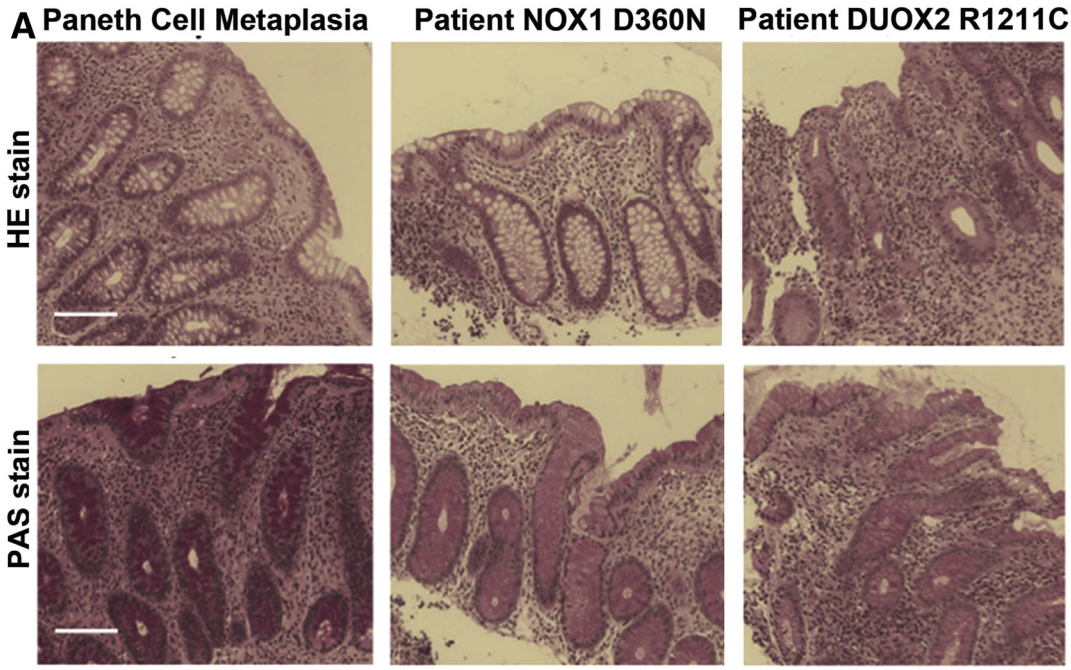
A
Paneth Cell Metaplasia
Patient NOX1 D360N
Patient DUOX2 R1211C
HE stain
PAS stain

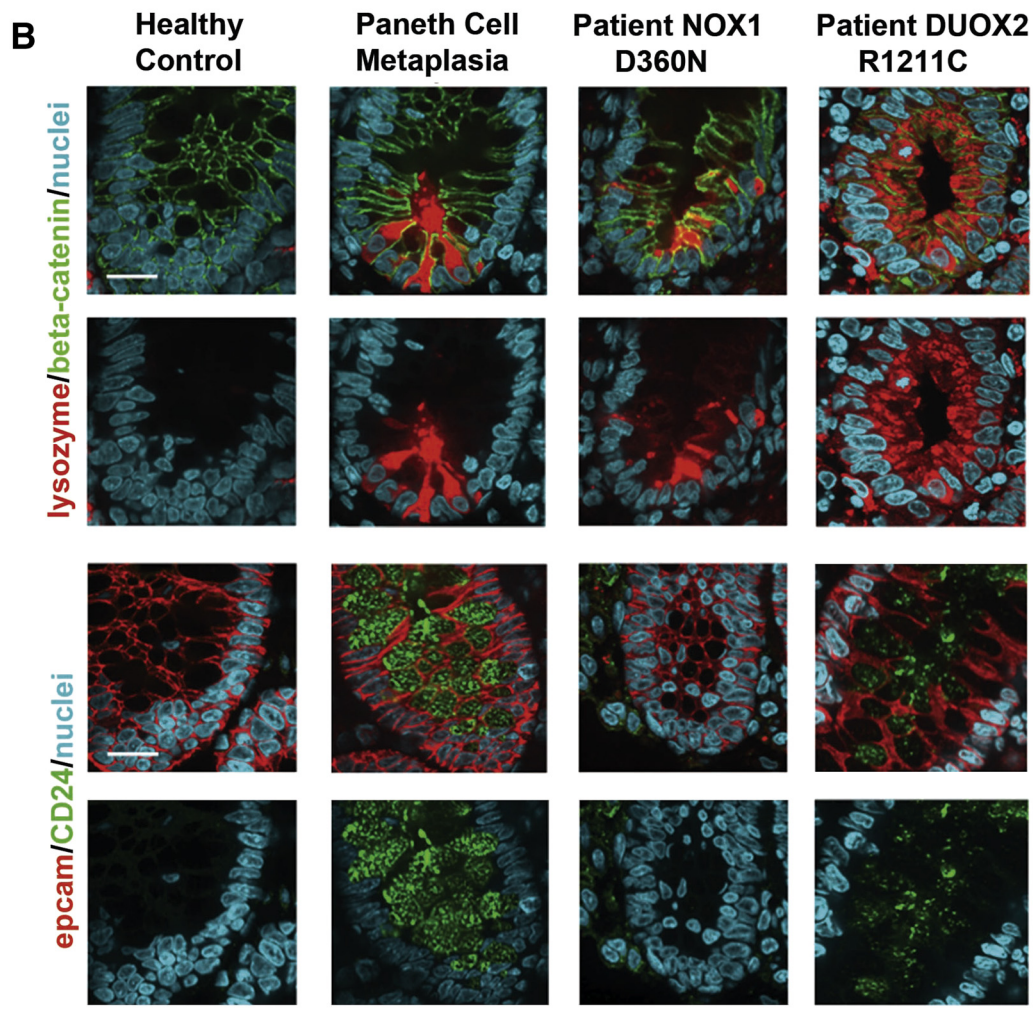
B
Healthy Control
Paneth Cell Metaplasia
Patient NOX1 D360N
Patient DUOX2 R1211C
lysozyme/beta-catenin/nuclei
epcam/CD24/nuclei

grown *C. jejuni* 81-176 was washed and resuspended in tissue culture medium at OD_{600}= 0.4 and added at multiplicity of infection 1000 to cells, followed by centrifugation at 250*g* for 5 minutes. After incubation for 3 hours at 37°C, the nonadherent and cell-associated bacteria were collected. For invasion, the infected and washed monolayers were incubated further with and without gentamicin (400 μg/mL) and incubated for an additional 2 hours at 37°C. The cells were lysed by the addition of 0.1% Triton X-100 in PBS for 10 minutes at 37°C. Bacterial counts for each assay were enumerated by serial dilution plating. All parameters were calculated as the average of the total number of colony-forming units/total initial inoculum.

Statistical Analysis

All functional experiments were conducted in triplicate with three repeats (n = 3), followed by an unpaired Student's *t* test.

Results

Identification of NOX1 and DUOX2 Variants in VEOIBD

NOX1 and *DUOX2* missense mutations were identified in five of 59 VEOIBD patients (age ≤6 years). All five patients presented with pancolitis without small bowel or perianal disease at diagnosis. None of the patients had systemic disease including thyroid disease or chronic infections, suggesting that defects were confined to the intestinal epithelium. SNPs and insertion/deletion variants were confirmed using Sanger sequencing and analyzed for potential function. Exon sequencing (Table 1–2) identified a novel *NOX1* variant (c.988G>A; p.P330S) in one male patient. Another rare variant (c.967G>A; rs34688635; p.D360N) was found in one male and one female patient. The missense variant NOX1 p.P330S is potentially damaging (Polyphen2 score: 0.995) and unique according to the Washington Exome Variant Server, while NOX1 p.D360N was predicted to be "probably damaging" by PolyPhen2 and was given a maximum evolutionary conservation score of 1 by the PhastCons program using 46 mammalian species. Variants in *DUOX2* were also identified in VEOIBD patients (Table 1–2). One of the patients was heterozygous for DUOX2 p.R1211C (c.4474G>A) and developed severe disease that necessitated colonic resection. The disease subsequently recurred at the resection site, a finding consistent with Crohn's disease. The second variant was detected in a very early onset UC patient heterozygous for DUOX2 p.R1492C (c.3631C>T; rs374410986), who presented with pancolitis.

In an independent replication cohort of 150 VEOIBD patients, none of the *NOX1* and *DUOX2* missense variants were identified. Similarly, in the publicly available International IBD Genetics Consortium (http://www.ibdgenetics.org) database none of the NOX1 and DUOX2 missense mutations were identified as this data set does not examine rare variants, only common polymorphisms, and the p.Asp360Asn variant is not analyzed by the immunochip.

Therefore, we took an alternate approach employing an array-based genotyping using the Illumina HumanExome v1.0 platform of 1477 Crohn's disease (CD) cases, 559 UC cases, and 2614 healthy controls, all with genetically verified Ashkenazi Jewish (AJ) ancestry by principal components analysis. Using this approach we detected association with UC in males at p.D360N in *NOX1* (MAF_{case} = 3.37%, $MAF_{control}$ = 0.82%; odds ratio 4.22; $P = 1.25 \times 10^{-3}$). The association was not detected in either of the female AJ UC cases (MAF_{case} = 1.53%, $MAF_{control}$ = 0.99%; odds ratio 1.55; P = .343), although the trend was in the same direction as observed in the AJ males cases. However, this trend was not observed in Crohn's disease cases (MAF_{CD} = 0.97%). The finding in an adult UC cohort suggests that pathways/processes involved in VEOIBD will have implications for adult IBD patients.

Histologic Analysis of NOX1/DUOX2 Variants

Histopathology analysis using HE and PAS staining (Figure 1*A*) was performed in biopsies from patients with the identified DUOX2 p.R1211C variant as well as a patient with the NOX1 p.D360N variant and compared with the healthy control and an IBD control biopsy. The disease control showed features of chronic and regenerative IBD, demonstrated by metaplastic Paneth cells within colonic crypts. The patient with the NOX1 p.D360N variant showed focal inflammation, increased cellularity of inflammatory cells adjacent to normal areas of unaffected colonic mucosa. The patient with the DUOX2 p.R1211C variant demonstrated more severe morphologic changes, with severe inflammation and crypt damage in the colonic mucosa when compared with the NOX1 variant.

Immunofluorescence staining was performed on colonic biopsy samples to determine whether Paneth cell metaplasia, a feature of chronic and regenerative change as a consequence of continuous inflammation within the colon, has occurred. Both markers, lysozyme and CD24, were highly positive in metaplastic Paneth cells of colonic crypt enterocytes in the disease control (see Figure 1*B*).

Figure 1. (*See previous page*). Characterization of selected patient biopsies. (*A*) HE and periodic acid–Schiff staining of colonic biopsy samples from an inflammatory bowel disease (IBD) control (Paneth cell metaplasia), a patient with the *NOX1* D360N variant, and a patient with the *DUOX2* R1211C variant. The patient with the *NOX1* D360N variant shows focal inflammation, increased cellularity of inflammatory cells adjacent to normal area. The patient with the *DUOX2* R1211C variant shows severe colitis with architectural distortion (crypt damage). Scale bar: 20 μm. (*B*) Immunofluorescence analysis with Paneth cell markers lysozyme and CD24 in colonic biopsy samples: lysozyme and EpCAM (*red*), β-catenin and CD24 (*green*), and nuclei (*blue*). Lysozyme was expressed in the crypts of the patients as well as the IBD control, but not in the healthy control. CD24 is expressed in colonic crypts in the IBD control and the patient with the *DUOX* R1211C variant, but neither in the healthy control nor the patient with the *NOX1* variant. Scale bar: 10 μm.

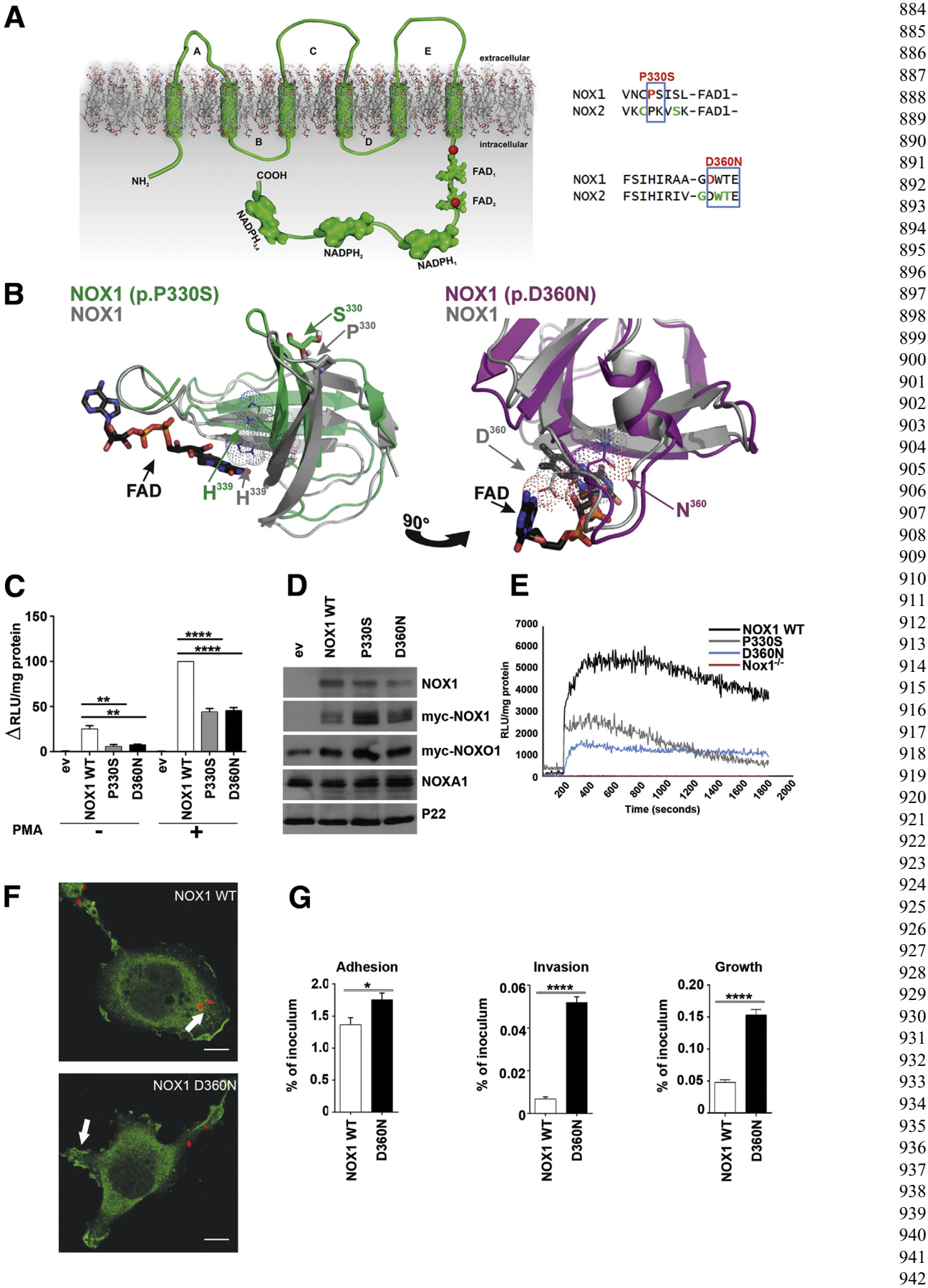
A
extracellular
intracellular
A
B
C
D
E
NH2
COOH
FAD1
FAD2
NADPH3
NADPH2
NADPH1
P330S
NOX1 VNCPSISL-FAD1-
NOX2 VKCPKVSK-FAD1-
D360N
NOX1 FSIHIRAA-GDWTE
NOX2 FSIHIRIV-GDWTE
B
NOX1 (p.P330S)
NOX1
S330
P330
FAD
H339
H339
NOX1 (p.D360N)
NOX1
D360
FAD
N360
90°
C
ΔRLU/mg protein
150
100
50
0
**
**
****
****
ev
NOX1 WT
P330S
D360N
ev
NOX1 WT
P330S
D360N
PMA
-
+
D
ev
NOX1 WT
P330S
D360N
NOX1
myc-NOX1
myc-NOXO1
NOXA1
P22
E
RLU/mg protein
7000
6000
5000
4000
3000
2000
1000
0
NOX1 WT
P330S
D360N
Nox1-/-
200
400
600
800
1000
1200
1400
1600
1800
2000
Time (seconds)
F
NOX1 WT
NOX1 D360N
G
Adhesion
% of inoculum
2.0
1.5
1.0
0.5
0
*
NOX1 WT
D360N
Invasion
% of inoculum
0.06
0.04
0.02
0
****
NOX1 WT
D360N
Growth
% of inoculum
0.20
0.15
0.10
0.05
0
****
NOX1 WT
D360N

Altered NOX1 appears not to progress cells into full metaplasia as seen by the absence of CD24 within crypt cells of the patient harboring NOX1 p.D360N. In colonic crypts of the patient with the DUOX2 p.R1211C variant, both lysozyme and CD24 were expressed, albeit not as prominent as observed within metaplastic Paneth cells in the IBD control.

Topologic Models of NOX1/DUOX2 Variants

The NOX1 NADPH oxidase is formed by heterodimerization of NOX1 with $p22^{phox}$, followed by assembly with the regulatory proteins NOXO1, NOXA1, and Rac1-GTP.[8] The cytosolic carboxyl terminus of NADPH oxidases harbors NADPH and FAD-binding regions, which are required for electron transport across the membrane via hemes where molecular oxygen is reduced to form superoxide. The identified NOX1 variants are located either just in front of FAD_1 (p.P330S) or inside FAD_2 (p.D360N) (Figure 2*A*). Pro330 and Asp360 are conserved in NOX1–4 proteins identified in vertebrates and lower organisms. *CYBB* missense variants (X-CGD) leading to loss or diminished ROS generation in neutrophils are located in close vicinity to the identified NOX1 variants (http://bioinf.uta.fi/CYBBbase).[36] Modeling of NOX1 WT, NOX1 (p.P330S), or NOX1 (p.D360N) dehydrogenase domains was performed by combining the crystal structures of FAD-binding domains homologous to the NOX FAD with the partial structure of the dehydrogenase domain of NOX2 in the correct orientation (see Figure 2*B*).

FAD and NADPH were docked to each NOX/DUOX model by using HADDOCK. FAD binds to NOX1 WT mainly with electrostatic interaction to His339 in the FAD_1 domain and Asp360 in the FAD_2 domain. Based on the model, Pro330 will be important for stabilization of the antiparallel β-structure that creates the FAD_1 domain. Although Pro330 is not directly involved in FAD binding, the change Pro330Ser in NOX1 alters the position of His339 in the FAD_1 domain, which decreases binding affinity of this variant for FAD.

The second NOX1 residue altered in VEOIBD, Asp360, is directly involved in FAD binding, and therefore a change to asparagine (D360N) weakens the interaction between FAD and NOX1. FAD binds to NOX1 with binding affinity in μM range; therefore, we predict that small structural changes in both FAD domains will compromise catalytic activity of the NOX1 enzyme. Debeurme et al[37] reported disrupted FAD binding and diminished catalytic activity of NOX2 in selected *CYBB* variants.

Functional Characterization of NOX1 Variants

As structural analysis predicts that the catalytic activity of NOX1 variants will be compromised, we reconstituted WT and altered NOX1 complexes in an epithelial model cell system (Cos7) deficient in all NOX/DUOX isoforms. Both NOX1 p.P330S and NOX1 p.D360N variants displayed diminished catalytic activity (see Figure 2*C*). Basal and phorbol ester-stimulated ROS generation was significantly reduced for NOX1 missense variants (50%–60%), and the overall protein expression was comparable to WT NOX1 (see Figure 2*D*).

As patients could not be recalled for colon tissue evaluation, catalytic activity of NOX1 variants was also measured in a murine in vivo expression setting. Nox1 knockout mice were transduced with lentivirus encoding NOX1 WT and variants intrarectally, and ROS generation of isolated crypts was recorded 24 hours later. Similar to the results obtained in cell lines, ROS production in the crypts was reduced in the NOX1 variants when compared with NOX1 WT (see Figure 2*E*).

A reduction in epithelial ROS production will attenuate host protection from intestinal pathogens. Defective processing of responses to mucosal bacteria is recognized to play a central role in the development and perpetuation of intestinal inflammation in IBD. *C. jejuni* in particular has been associated with the initiation of IBD.[38] *C. jejuni* uptake was used to visualize infection-associated translocation of NOX1 to membrane ruffles and to assess the antibacterial response.[10] Stimulated membrane localization of NOX1 WT and NOX1 variants (NOX1 p.D360N shown) were comparable (see Figure 2*F*), but reduced ROS generation caused a 10-fold increase in bacterial invasion when cells harbored the NOX1 p.P330S or NOX1 p.D360N variants with reduced catalytic activity (see Figure 2*G*).

Functional Characterization of DUOX2 Variants

Inactivating mutations in *DUOX2* or *DUOXA2* have been linked to inherited permanent or transient congenital hypothyroidism,[39] and to date over 23 *DUOX2* mutations have been described in this context (HGMD, www.hgmd.cf.ac.uk/ac/gene) (Figure 3*A*). The two VEOIBD-associated *DUOX2* variants are novel; in contrast to most of the reported *DUOX2* variants, they not located in the peroxidase homology domain or the EF hand regions. DUOX2 p.R1221C is placed in a polybasic region within an intracellular loop, and Arg1492 in DUOX2 is an integral part of the highly

Figure 2. (*See previous page*). Modeling and functional characterization of *NOX1* variants. (*A*) Topologic model depicting *NOX1* very early onset inflammatory bowel disease (VEOIBD) variants (*red*), selected X-CGD *CYBB* (NOX2) variants (*green*), conserved residues (*blue*). (*B*) Three-dimensional model of NOX1 wild-type (WT) (*grey*), NOX1 P330S (*green*), or NOX1 D360N (*pink*) dehydrogenase domains. NADPH, FAD, residue H339, and variant positions are marked. (*C*) ROS production by *NOX1* WT and variants. (*D*) Protein expression of NOX1 and variants, Myc-NOXO1, NOXA1, and $p22^{phox}$ as loading control. (*E*) ROS production in murine $Nox1^{-/-}$ crypts transduced with NOX1 WT or variants. Phorbol 12-myristate 13-acetate (PMA) stimulation was at 200 seconds. (*F*) Localization of Myc-NOX1 WT or D360N (*green*) in *C. jejuni* (red) infected Cos-p22 cells. Scale bar: 10 μm; arrow indicates membrane localization. (*G*) Adhesion and invasion of *Campylobacter jejuni* in cells expressing NOX1 WT, P330S, or D360N. Error bars ± standard deviation n = 3; $^{*}P \leq .05$; $^{**}P \leq .01$; $^{****}P \leq .0001$; comparing *NOX1* WT to variants.

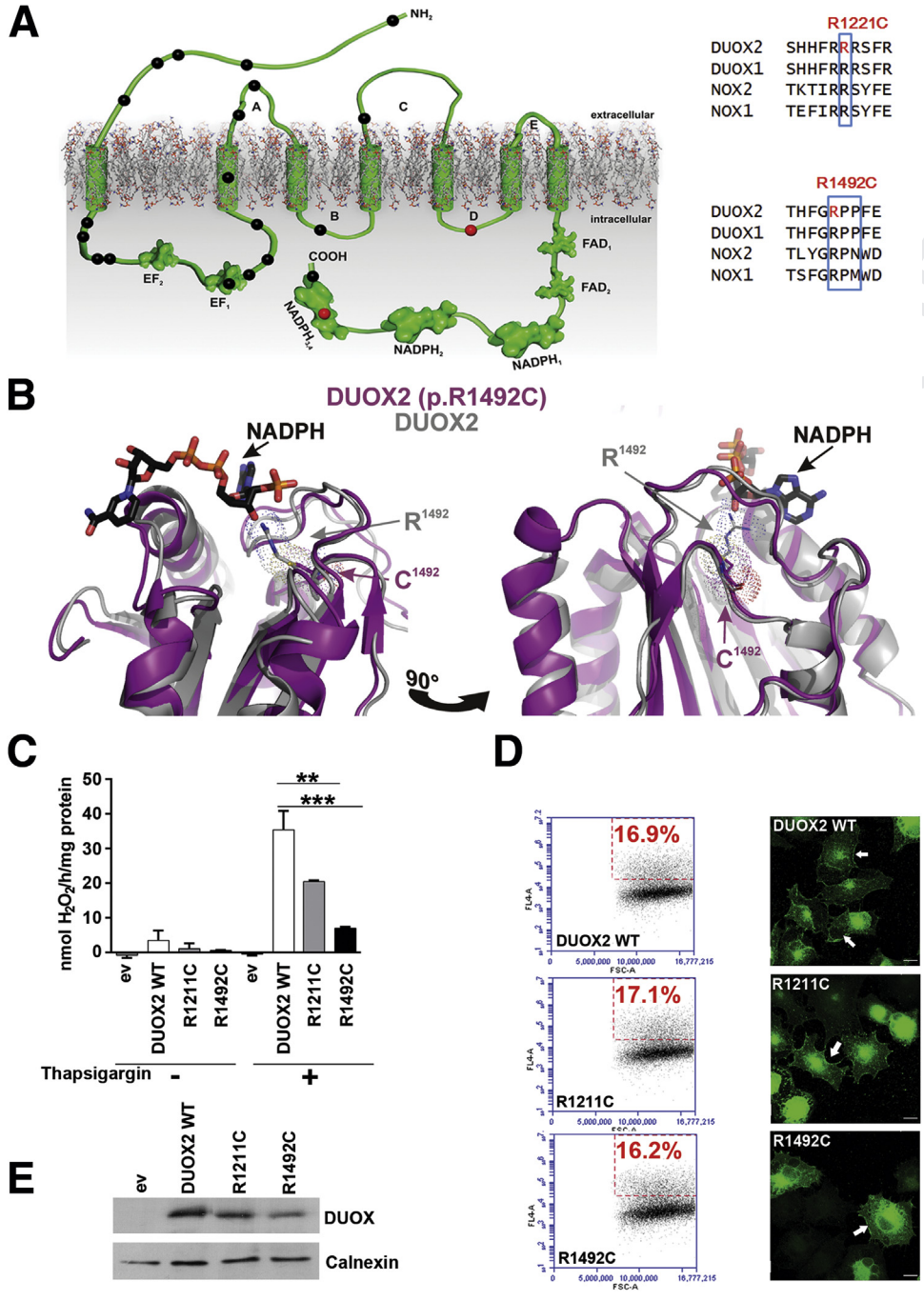

Figure 3. Modeling and functional characterization of *DUOX2* variants. (*A*) Topologic model depicting *DUOX2* very early onset inflammatory bowel disease (VEOIBD) variants (*red*), selected *DUOX2* hypothyroidism variants (*black*), and conserved residues (*blue*). (*B*) Three-dimensional model of DUOX2 wild-type (WT) (*grey*) and DUOX2 R1492C (*pink*) dehydrogenase domain. NADPH, FAD, and variant position are marked. (*C*) H_2O_2 release by DUOX2 WT and variants. (*D*) Protein expression of HA-DUOX2 WT and variants; calnexin served as loading control. (*E*) HA-DUOX2 WT and variant surface expression by flow cytometry (*left*) and localization by immunofluorescence (*right*) (*green*, *arrow* for membrane). Scale bar: 10 μm. (*F*) Adhesion and invasion of *C. jejuni* in cells expressing HA-DUOX2 WT, R1211C, or R1492C. Error bars ± standard deviation, n = 3; *$P \leq .05$; **$P \leq .01$; ***$P \leq .001$; ****$P \leq .0001$; comparing DUOX2 WT with variants.

web 4C/FPO

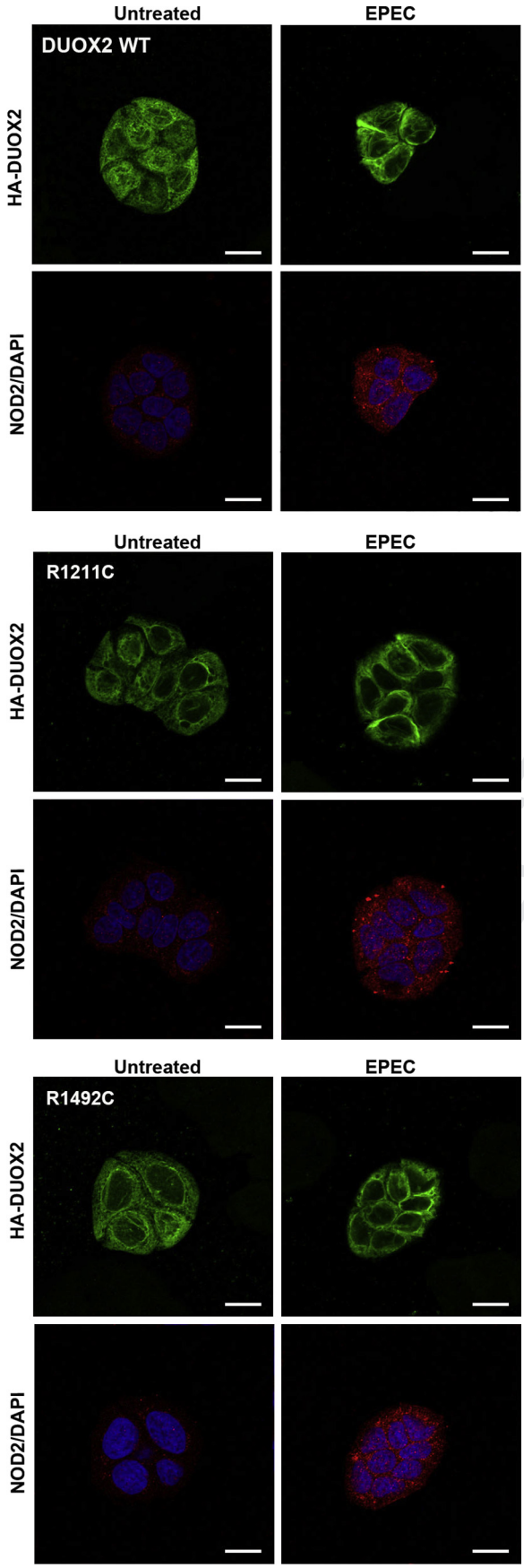

conserved GRP sequence in the $NADPH_3$ domain (see Figure 3*A*).

As described for NOX1, the dehydrogenase domains of DUOX2 WT and DUOX2 p.R1492C were modeled onto the extended NOX2 structure; by use of HADDOCK, NADPH and FAD were docked to the structure (see Figure 3*B*). Structural analysis revealed that Arg1492 is part of the NADPH-binding pocket. NADPH binds to DUOX2 WT with strong electrostatic interactions to the residues Arg1421 and Arg1492 with a sum of -181.7 ± 76.4 kcal/mol and with weak Van der Waals interactions to Gly1385, Thr1463, Pro1520, Gly1521, and Met1520 with a sum of -30.9 ± 7.8 kcal/mol. Replacing Arg1492 with cysteine as in the DUOX2 p.R1492C variant does not change the DUOX2 structure or the position of other NADPH-interacting residues. However, the change is predicted to weaken the interaction between NADPH and DUOX2 by a factor of 2. How replacement of Arg1221 with cysteine will directly affect DUOX2 catalytic activity cannot be predicted because suitable structures for modeling do not exist, but in both NOX2 and NOX4 the analogous D loop participates in ROS production.[40,41]

Functional analysis of DUOX2 variants was performed in the H661 cellular model system that represents a physiologic context for DUOX-DUOXA expression and is devoid of NOX1–5 activity.[29] Both DUOX2 variants, when coexpressed with their dimerization partner DUOXA2, produced significantly less H_2O_2 than WT DUOX2 (see Figure 3*C*), although protein expression and cellular localization were not altered (see Figure 3*D* and *E*). DUOX2 has been functionally associated with NOD2 in transient overexpression conditions.[42] HT29 colonic cells express endogenously functional NOX1 complex and NOD2, and thus provide an appropriate context for analysis of putative DUOX2-NOD2 interactions.

DUOX2 or DUOX2 variants together with DUOXA2 were stably incorporated into HT29 cells, followed by exposure to enteropathogenic *E. coli*. DUOX2 WT or variants, localized on internal membrane structures before the challenge, translocated to the plasma membrane and cell-cell junctions. NOD2, on the other hand, remained in the intracellular compartment, albeit NOD2 protein expression was upregulated (Figure 4). Thus, DUOX2 and NOD2 were not recruited simultaneously upon *E. coli* challenge.

Stimulated H_2O_2 release in DUOX2 WT or variant-expressing HT29 cells mirrored the results obtained with H661 cells (data not shown). DUOX2-mediated H_2O_2 release at apical membranes has been linked to antimicrobial host defense and decreased *C. jejuni* virulence.[10] Comparison of *C. jejuni* invasion in DUOX2 WT or DUOX2 variant-expressing (DUOX2 p.R1211C, DUOX2 epithelial cells showed increased invasion when ROS generation was diminished (see Figure 3*F*).

Figure 4. Bacteria-induced translocation of DUOX2 and variants does not involve NOD2 in colonic cells. HT29 cells stably expressing DUOX2 WT, DUOX2 R1211C, and DUOX2 R1492C were exposed to enteropathogenic *Escherichia coli* (EPEC) for 5 hours. Immunofluorescence images of DUOX2 (*green*), NOD2 (*red*), and nuclei (*blue*). Scale bar: 15 μm.

Discussion

We have identified novel inactivating missense variants in each of the epithelial NADPH oxidases *NOX1* (p.P330S, p.D360N) and *DUOX2* (p.R1211C, p.R1492C) in five VEOIBD patients. Variants in X-linked *NOX1* were found in two male VEOIBD patients, and *NOX1* p.D360N was associated with male UC in an AJ ancestry case-control cohort, likely leading to increased or sustained disease severity.

The identification of rare functional variants contributing to the pathogenesis of VEOIBD has been observed with other genes, including the NOX2 NADPH oxidase complex,[7] *NOS2*,[43] *IL10R*,[15] and *XIAP*.[44,45] The variants we identified in both *NOX1* and *DUOX2* are rare and not found in a replication VEOIBD cohort or data sets of common variants. However, all variants showed both pathologic and functional defects, indicating that these variants may contribute to disease susceptibility or pathogenesis. Further large-scale sequencing of pediatric- and adult-onset IBD may indicate a broader role of both *NOX1* and *DUOX2* in IBD pathogenesis, as observed in our AJ population.

Recently, altered DUOX2 expression was identified in ileum biopsies from pediatric Crohn's disease patients.[46] Further, ROS derived from NADPH oxidases is critical to control mucin granule accumulation in colonic goblet cells,[12] and NOX1 has been shown to control the balance between goblet and absorptive cell types in murine colon.[47] Interestingly, colonic biopsies from patients carrying either *NOX1* p.D360N or *DUOX2* p.R1211C variants showed abnormal CD24 and lysozyme expression (see Figure 1*B*), suggesting a role for these proteins in Paneth cell metaplasia.

The thyroid function of the two male VEOIBD patients harboring *DUOX2* mutations was normal, although inactivating monoallelic and biallelic *DUOX2* and *DUOXA2* variants have been linked to hypothyroidism.[48] In contrast to adult onset IBD, VEOIBD frequently encompasses a unique clinical presentation, with severe disease limited to the colon and with poor response to standard therapies.[24] VEOIBD variants (*NCF2*,[49] *NOS2*,[43] *IL10RA/B*,[15] *TTC7A*[50]) have usually been rare, suggesting that these patients may have a unique genetic susceptibility. Furthermore, we have recently shown that SNPs and rare variants in all components of the NOX2 NADPH oxidase complex are associated with VEOIBD.[7] Similar to our recent observations with NOX2 NADPH oxidase complex variants leading to decreased ROS production in neutrophils,[7] reduced mucosal ROS levels originating from NOX1 and DUOX2 variants play also a role in susceptibility to VEOIBD and perhaps other severe IBD phenotypes.

Intestinal NADPH oxidases connect to antibacterial autophagy and endosomal pathways important for mucus secretion and may modulate the interplay between commensal bacteria and pathogens.[12,13] Recent microbiome studies on a large pediatric cohort with new-onset Crohn's disease assigned a unique role to changes in the rectal mucosal microbiota for disease classification.[51] Changes in ROS generation at the mucosal surface will most likely result in dysbiosis, intestinal inflammation, and pathobiont development. Our functional studies provide strong support both for the pathogenic nature of the mutations identified in these VEOIBD patients and the role of epithelial ROS in protecting cells from bacterial attack.

Further phenotypic exploration of *NOX/DUOX* variants will be aided by studies in humans and improved animal models, as current IBD animal models seem often not to reflect human disease triggered by reduced ROS. For example, murine *Cybb* (NOX2) deficiency does not lead to spontaneous Crohn's disease-like intestinal disease and gut inflammation, both observed in many CGD patients. Although *Cybb* knockout mice exhibit several hallmarks of CGD upon fungal or bacterial challenge, they were slightly protected in the dextran sodium sulfate–induced colitis mouse model.[52] Similarly, *Nox1* deficiency in the murine mucosa did not alter dextran sodium sulfate–colitis pathology,[53] although combined *Nox1* and *Il10* deficiency caused spontaneous colitis in mice.[54] Mice harboring an inactivating *Duox2* variant or *Duoxa* deficiency showed severe hypothyroidism and increased colonization with *Helicobacter felis*.[11,55]

In conclusion, our findings demonstrate that novel NOX1 and DUOX2 NADPH oxidase variants resulting in attenuated ROS production and impaired innate defense occur in children with VEOIBD. This may influence IBD pathogenesis beyond childhood.

References

1. Jostins L, Ripke S, Weersma RK, et al. Host-microbe interactions have shaped the genetic architecture of inflammatory bowel disease. Nature 2012;491:119–124.
2. Maloy KJ, Powrie F. Intestinal homeostasis and its breakdown in inflammatory bowel disease. Nature 2011; 474:298–306.
3. van den Berg JM, van Koppen E, Ahlin A, et al. Chronic granulomatous disease: the European experience. PLoS One 2009;4:e5234.
4. Marks DJ, Miyagi K, Rahman FZ, et al. Inflammatory bowel disease in CGD reproduces the clinicopathological features of Crohn's disease. Am J Gastroenterol 2009; 104:117–124.
5. Muise AM, Snapper SB, Kugathasan S. The age of gene discovery in very early onset inflammatory bowel disease. Gastroenterology 2012;143:285–288.
6. Somasundaram R, Deuring JJ, van der Woude CJ, et al. Linking risk conferring mutations in NCF4 to functional consequences in Crohn's disease. Gut 2012; 61:1097–1098.
7. Dhillon SS, Fattouh R, Elkadri A, et al. Variants in nicotinamide adenine dinucleotide phosphate oxidase complex components determine susceptibility to very early onset inflammatory bowel disease. Gastroenterology 2014;147:680–689.e2.
8. Lambeth JD, Neish AS. Nox enzymes and new thinking on reactive oxygen: a double-edged sword revisited. Annu Rev Pathol 2014;9:119–145.
9. Rada B, Leto TL. Oxidative innate immune defenses by Nox/Duox family NADPH oxidases. Contrib Microbiol 2008;15:164–187.

10. Corcionivoschi N, Alvarez LA, Sharp TH, et al. Mucosal reactive oxygen species decrease virulence by disrupting *Campylobacter jejuni* phosphotyrosine signaling. Cell Host Microbe 2012;12:47–59.
11. Grasberger H, El-Zaatari M, Dang DT, et al. Dual oxidases control release of hydrogen peroxide by the gastric epithelium to prevent *Helicobacter felis* infection and inflammation in mice. Gastroenterology 2013; 145:1045–1054.
12. Patel KK, Miyoshi H, Beatty WL, et al. Autophagy proteins control goblet cell function by potentiating reactive oxygen species production. EMBO J 2013;32: 3130–3144.
13. Jones RM, Luo L, Ardita CS, et al. Symbiotic lactobacilli stimulate gut epithelial proliferation via Nox-mediated generation of reactive oxygen species. EMBO J 2013; 32:3017–3028.
14. Little JL, Higgins PT, Ioannidis JPA, et al. STREGA: Strengthening the Reporting of Genetic Associations: an extension of the STROBE Statement. Ann Intern Med 2009;150 2009:206–215, Also available at: http://www.medicine.uottawa.ca/public-health-genomics/web/eng/strega.html.
15. Moran CJ, Walters TD, Guo CH, et al. IL-10R polymorphisms are associated with very-early-onset ulcerative colitis. Inflamm Bowel Dis 2013;19:115–123.
16. Muise AM, Walters T, Xu W, et al. Single nucleotide polymorphisms that increase expression of the guanosine triphosphatase *RAC1* are associated with ulcerative colitis. Gastroenterology 2011;141:633–641.
17. Adzhubei IA, Schmidt S, Peshkin L, et al. A method and server for predicting damaging missense mutations. Nat Methods 2010;7:248–249.
18. Kumar P, Henikoff S, Ng PC. Predicting the effects of coding non-synonymous variants on protein function using the SIFT algorithm. Nat Protoc 2009;4: 1073–1081.
19. Yuan HY, Chiou JJ, Tseng WH, et al. FASTSNP: an always up-to-date and extendable service for SNP function analysis and prioritization. Nucleic Acids Res 2006; 34:W635–W641.
20. Desmet FO, Hamroun D, Lalande M, et al. Human Splicing Finder: an online bioinformatics tool to predict splicing signals. Nucleic Acids Res 2009;37:e67.
21. Wang J, Ronaghi M, Chong SS, et al. pfSNP: An integrated potentially functional SNP resource that facilitates hypotheses generation through knowledge syntheses. Hum Mutat 2011;32:19–24.
22. Benchimol EI, Mack DR, Nguyen GC, et al. Incidence, outcomes, and health services burden of very early onset inflammatory bowel disease. Gastroenterology 2014; 147:803–813.e7.
23. Uhlig HH, Schwerd T, Koletzko S, et al. The diagnostic approach to monogenic very early onset inflammatory bowel disease. Gastroenterology 2014; 147:990–1007.e3.
24. Levine A, Kugathasan S, Annese V, et al. Pediatric onset Crohn's colitis is characterized by genotype-dependent age-related susceptibility. Inflamm Bowel Dis 2007; 13:1509–1515.
25. Uhlig HH. Monogenic diseases associated with intestinal inflammation: implications for the understanding of inflammatory bowel disease. Gut 2013;62:1795–1805.
26. Sali A, Blundell TL. Comparative protein modelling by satisfaction of spatial restraints. J Mol Biol 1993; 234:779–815.
27. De Vries SJ, van Dijk M, Bonvin AM. The HADDOCK web server for data-driven biomolecular docking. Nat Protoc 2010;5:883–897.
28. Van Dijk AD, Bonvin AM. Solvated docking: introducing water into the modelling of biomolecular complexes. Bioinformatics 2006;22:2340–2347.
29. Luxen S, Noack D, Frausto M, et al. Heterodimerization controls localization of Duox-DuoxA NADPH oxidases in airway cells. J Cell Sci 2009;122:1238–1247.
30. Yu L, Zhen L, Dinauer MC. Biosynthesis of the phagocyte NADPH oxidase cytochrome b558. Role of heme incorporation and heterodimer formation in maturation and stability of gp91phox and p22phox subunits. J Biol Chem 1997;272:27288–27294.
31. Pacquelet S, Lehmann M, Luxen S, et al. Inhibitory action of NoxA1 on dual oxidase activity in airway cells. J Biol Chem 2008;283:24649–24658.
32. Antony S, Wu Y, Hewitt SM, et al. Characterization of NADPH oxidase 5 expression in human tumors and tumor cell lines with a novel mouse monoclonal antibody. Free Radic Biol Med 2013;65:497–508.
33. von Lohneysen K, Noack D, Jesaitis AJ, et al. Mutational analysis reveals distinct features of the Nox4-p22 phox complex. J Biol Chem 2008;283:35273–35282.
34. Martyn KD, Frederick LM, von Loehneysen K, et al. Functional analysis of Nox4 reveals unique characteristics compared to other NADPH oxidases. Cell Signal 2006;18:69–82.
35. Elsinghorst EA. Measurement of invasion by gentamicin resistance. Methods Enzymol 1994;236:405–420.
36. Kuhns DB, Alvord WG, Heller T, et al. Residual NADPH oxidase and survival in chronic granulomatous disease. N Engl J Med 2010;363:2600–2610.
37. Debeurme F, Picciocchi A, Dagher MC, et al. Regulation of NADPH oxidase activity in phagocytes: relationship between FAD/NADPH binding and oxidase complex assembly. J Biol Chem 2010;285:33197–33208.
38. Gradel KO, Nielsen HL, Schonheyder HC, et al. Increased short- and long-term risk of inflammatory bowel disease after salmonella or campylobacter gastroenteritis. Gastroenterology 2009;137:495–501.
39. Moreno JC, Bikker H, Kempers MJ, et al. Inactivating mutations in the gene for thyroid oxidase 2 (*THOX2*) and congenital hypothyroidism. N Engl J Med 2002; 347:95–102.
40. Carrichon L, Picciocchi A, Debeurme F, et al. Characterization of superoxide overproduction by the D-Loop(Nox4)-Nox2 cytochrome b(558) in phagocytes—differential sensitivity to calcium and phosphorylation events. Biochim Biophys Acta 2011; 1808:78–90.
41. Von Lohneysen K, Noack D, Wood MR, et al. Structural insights into Nox4 and Nox2: motifs involved in function and cellular localization. Mol Cell Biol 2010;30:961–975.

42. Lipinski S, Till A, Sina C, et al. *DUOX2*-derived reactive oxygen species are effectors of *NOD2*-mediated antibacterial responses. J Cell Sci 2009;122: 3522–3530.
43. Dhillon SS, Mastropaolo LA, Murchie R, et al. Higher activity of the inducible nitric oxide synthase contributes to very early onset inflammatory bowel disease. Clin Transl Gastroenterol 2014;5:e46.
44. Latour S, Aguilar C. XIAP deficiency syndrome in humans. Semin Cell Dev Biol 2015;39:115–123.
45. Speckmann C, Ehl S. XIAP deficiency is a mendelian cause of late-onset IBD. Gut 2014;63:1031–1032.
46. Haberman Y, Tickle TL, Dexheimer PJ, et al. Pediatric Crohn disease patients exhibit specific ileal transcriptome and microbiome signature. J Clin Invest 2014; 124:3617–3633.
47. Coant N, Ben Mkaddem S, Pedruzzi E, et al. NADPH oxidase 1 modulates WNT and NOTCH1 signaling to control the fate of proliferative progenitor cells in the colon. Mol Cell Biol;30:2636–2650.
48. Muzza M, Rabbiosi S, Vigone M, et al. The clinical and molecular characterization of patients with dyshormonogenic congenital hypothyroidism reveals specific diagnostic clues for *DUOX2* defects. J Clin Endocrinol Metab 2014;99:E544–E553.
49. Muise AM, Xu W, Guo CH, et al. NADPH oxidase complex and IBD candidate gene studies: identification of a rare variant in NCF2 that results in reduced binding to *RAC2*. Gut 2012;61:1028–1035.
50. Avitzur Y, Guo C, Mastropaolo LA, et al. Mutations in tetratricopeptide repeat domain 7A result in a severe form of very early onset inflammatory bowel disease. Gastroenterology 2014;146:1028–1039.
51. Gevers D, Kugathasan S, Denson LA, et al. The treatment-naive microbiome in new-onset Crohn's disease. Cell Host Microbe 2014;15:382–392.
52. Bao S, Carr ED, Xu YH, et al. Gp91(phox) contributes to the development of experimental inflammatory bowel disease. Immunol Cell Biol 2011;89:853–860.
53. Leoni G, Alam A, Neumann PA, et al. Annexin A1, formyl peptide receptor, and *NOX1* orchestrate epithelial repair. J Clin Invest 2013;123:443–454.
54. Treton X, Pedruzzi E, Guichard C, et al. Combined NADPH oxidase 1 and interleukin 10 deficiency induces chronic endoplasmic reticulum stress and causes ulcerative colitis-like disease in mice. PLoS ONE 2014;9:e101669.
55. Johnson KR, Marden CC, Ward-Bailey P, et al. Congenital hypothyroidism, dwarfism, and hearing impairment caused by a missense mutation in the mouse dual oxidase 2 gene, *Duox2*. Mol Endocrinol 2007;21:1593–1602.

Received July 30, 2014. Accepted June 3, 2015.

Correspondence
Address correspondence to: Aleixo Muise, MD, PhD, Division of Gastroenterology, Hepatology, and Nutrition, Department of Pediatrics, University of Toronto, Hospital for Sick Children, Toronto, ON, Canada. e-mail: aleixo.muise@sickkids.ca.

Acknowledgments
The authors thank N. Corcionivoschi for technical assistance.

Conflicts of interest
These authors disclose the following: Scott B. Snapper has received personal fees from Pfizer, Ironwood Pharmaceuticals, AbbVie, and Cubist, outside of the submitted work. Holm H. Uhlig is participating in ongoing project collaborations or reagent supply unrelated to the manuscript, including UCB Pharma, Eli Lilly, GSK, Tetralogics, Vertex, and MSD. The remaining authors disclose no conflicts.

Funding
This study was funded by the Science Foundation Ireland (PI award, Stokes award to U.G.K.); the Children's Medical and Research Foundation Ireland (to B.B., U.G.K.); National Institutes of Health grants DK062413, AI067068, DK046763, HS021747, the European Union, the CCFA, and the Lisa Z and Joshua L Greer Endowed Chair in IBD Genetics (to D.P.B.M.); the New York Crohn's Foundation grant (to I.P.); National Institutes of Health grants U01 DK062429, DK062422, R01 DK092235, and the Ward-Coleman Translational Genetics Chair (to J.H.C.); the Medical Research Fund, Oxford (to H.U.); National Institutes of Health gratn DK62431, the Atran Foundation, and the Morton Hyatt Family (to S.R.B.); Crohn's and Colitis Canada (CCC), Canadian Association of Gastroenterology (CAG), and Canadian Institute of Health Research (CIHR) Fellowship (to A.E.); the RESTRACOMP fellowship from the Research Institute of the Hospital for Sick Children, Toronto, Canada (to C.T.); a CIHR–Operating Grant MOP119457 and MOP97756 (to A.M.M. and J.H.B.); and in part by Leona M. and Harry B. Helmsley Charitable Trust (to A.M.M., H.H.U., D.P.B.M., S.B.S., J.C.). Q1